NITROGEN-DOPED CARBON FOR LITHIUM-ION BATTERIES

Jinle Lan[1*], Yuan Liu[1], Yunhua Yu [1], Xiaoping Yang[1]

[1]College of Materials Science and Engineering, Beijing University of Chemical Technology, Beijing 100029, P.R.China , *E-mail: lanjl@mail.buct.edu.cn

Keywords: Polydopamine-based, N-doped carbon tubes, Hollow structure, Rate performance, Li-ion batteries

ABSTRACT

Three 1D polymer-derived amorphous carbons are prepared by electrospinning technique combined with SiO_x-template method in this section: polyacrylonitrile (PAN)-derived CNF, polyvinylpyrrolidone (PVP)-derived porous CNF, and Polydopamine (PDA)-derived N-doped carbon tube (N-CT). At first, the effect of N-doping on the electrochemical performance of PAN-derived CNF is investigated. The results show that N element content dercease from 12.5 at.% to 2.8 at.% with the carbonization temperature increased. The N types in the CNF are divided into tpyridinic N, pyridonic N, and graphitic N, respectively. Among the three N types, graphitic N contributes to the improvement of electron conductivity of CNF, thus enhancing the rate performance of CNF. Then, we evaluate the PVP-derived porous CNF as the anode materials for LIBs. It is found that hollow-structural pore are more beneficial for the penetration of Li^+-carrying electrode into the CNF, thus decreasing the Li^+-diffusion distance, which leads to improved electrochemical performance, especially the rate performance. At last, based on the aforementioned two works, we employ PDA as the precursor to prepare N-CT with an ultra-thin wall thickness of about 16 nm. The results shows that the graphitic N content in N-CT (carbonization temperature is 750℃) is abundant (~3.1%). Benefiting from the synergistic effect of unique hollow structure and abundant N-doping that shorts the Li^+-diffusion distance and facilitates the electron conductivity, the optimal N-CT electrode shows excellent rate performance (406 mA h g^{-1} at 2 A g^{-1}).

1 INTRODUCTION

In recent years, rechargeable lithium-ion batteries (LIBs) have been widely used in portable electronic devices and are regarded as one of the most promising energy storage/conversion devices for electric vehicles (EVs) and smart grids due to their unmatchable combination of high energy and power density, long cycle life and non-memory effect [1-3]. As one of the most important components in LIBs, anodes play a significant role in determining the overall performance. Though the most successfully commercialized anode material is graphite, increasing industrial demand for high-capacity power sources has led to further development of new anode materials as replacements for graphite in Li-ion batteries because of its low theoretical specific capacity(372 mAh/g) [4]. Owing to their variety, tunable specific capacity and rate capability, nanostructured carbonaceous materials have been considered as the most potential anode materials for high-performance LIBs.

A variety of nanostructured carbonaceous materials such as carbon nanotubes[5,6], carbon nanofibers[7,8], graphene[9-11], hollow carbon nanospheres[12,13] and their composites[14-16] have

been investigated as anode materials for LIBs. Among them, hollow structured carbonaceous materials have attracted considerable attention because the hollow structure can offer a high surface area, a large electrode/electrolyte interface and a shortened Li ion diffusion path[12,13,17]. For instance, an ensemble of monodisperse hollow carbon nanospheres with a shell thickness of ~12nm were synthesized via a combined polystyrene latex/hydrothermal carbonization templating approach, and showed high rate performance[12]. Recently, nitrogen-doped porous interconnected double-shelled HCSs prepared by chemical treatment of Fe_3O_4 @C precursors using HNO_3 delivered a remarkably high reversible capacity of 512 mA h g^{-1} at 1.5C after 500 cycles[18]. The obvious enhancement of electrochemical performance can be attributed to the enhanced electric conductivity and increased active sites.[19-23]. Therefore, it is worth looking forward to exploring new nitrogen-doped hollow structured carbon materials that can meet the demand of high energy and power densities.

Generally speaking, here are two main approaches to achieve the introduction of nitrogen atoms into carbon materials. One is post-treatment, such as HNO_3-impregnating treatment[24]and annealing with NH_3[25]. Another is in-situ doping through pyrolyzing nitrogen-containing organics[26]. Comparatively speaking, the latter one is believed to be relatively simple and eco-friendly method to prepare N-doped carbon materials. As a nitrogen-rich biomimetic polymer, polydopamine contains both catechol and amine groups, it is advantageous to electrolyte wetting, electrolyte uptake, and ionic conductivity[27,28] and can highly buffer the volume expansion of these high-capacity lithium-storage materials and improve the conductivity of the overall electrode during cycling when used as the in situ N-doped carbon precursor for coating SnO_2[29,30], MnO[31], Fe_3O_4[32,33], etc. However, to the best of our knowledge, the electrochemical properties of PDA-derived hollow-structured carbons have not been thoroughly evaluated as anode materials. More importantly, the structure and electrical conductivity of PDA-derived nitrogen-enriched carbon is similar to that of N-doped multi-layered graphene, which reveals huge potential for lithium-storage.

In this paper, we fabricated PDA-derived N-doped carbon tubes(N-CTs) through a template-assisted method and investigated its electrochemical performance as a lithium-ion battery anode material. Owing to the hollow nanostructure and nitrogen doping, the N-CT electrode showed a high initial reversible capacity of 753 mA h g^{-1} at 100 mA g^{-1}, and excellent rate performance (e.g., 406 mA h g^{-1} at 2 A g^{-1}).It is worth noting that the capacity significantly increased during the long-term cycling after the first several cycles. We believe that interlamellar spacing expansion led to easier insertion/extraction of Li ions into/from the inner part of the N-CTs, owing to the increase of active sites caused by the increased distance between adjacent layers, the capacity significantly improved.

2 EXPERIMENT

2.1 Synthesis of a silica nanofiber (SiO2 NFs) template

The SiO_2 NFs were synthesized by electrospinning with tetraethylorthosilicate (TEOS) as the silica precursor, followed by calcination in air[34]. Typically, 0.8 g of TEOS was added dropwise to 7ml N,N-dimethylformamide/acetic acid (volume ratio of 15/1) solvent mixture to form a homogenous solution. Then, 1 g of polyvinylpyrrolidone(PVP, Mw=1300000)was dissolved in the solution under vigorous stirring for 10 h to obtain the precursor solution for further electrospinning. The precursor solution was delivered to a stainless steel needle with an inner diameter of 0.5mm by using a syringe

pump and electrospun at a voltage of 25 kV. As-electrospun nanofibers were collected on the electrically grounded aluminum foil that covered the roller with a rotation speed of 600 rpm. Finally, SiO_2 nanofibers were obtained after calcination in air at 600 ℃ for 6h.

2.2 Synthesis of N-doped carbon tubes

100 mg of the as-prepared SiO_2 NFs were dispersed in 100 ml Tris-buffer (pH: ~8.5) by ultrasonication for 30 min to form a suspension. Then 100 mg dopamine was added to the suspension under stirring, After 10h of reaction, brown precipitates were obtained by centrifugation, washed several times with deionized water, and then dried at 60 ℃ in an vacuum oven for 12 h. Subsequently, the core-shell nanofibers were carbonized at 750 ℃ for 3h in a N_2 atmosphere. Finally, N-doped carbon tubes were obtained by etching off silica template with NaOH solution.

2.3 Characterization

a field emission scanning electron microscope (FE-SEM, Supra55, Carl Zeiss), a high resolution transmission electron microscope (HR-TEM, Tecnai G2F30S-TWIN), a wide angle X-ray diffractometer (XRD) (WAXD, D8 Advance, Bruker, Cu Kα, λ = 0.154 nm) and a Raman spectrometer (Renishaw, INVIA). An X-ray photoelectron spectrometer (XPS, EscaLab 250, Thermo Fisher Scientific) were used to analyzed the morphology, structure and the elemental chemical status of the sample.

2.4 Electrochemical measurements

The N-CT sample was mixed with carbon black and poly-(vinylidene difluoride) (PVDF) to form a slurry at a weight ratio of 7:2:1 in N-methyl pyrrolidone (NMP). The working electrode was prepared by casting the slurry onto nickel foil through a doctor blade method and then dried in a vacuum oven at 120 ℃ overnight, the cells were assembled in an Ar-filled glovebox with the mass loading of the active material for each electrode controlled to be about 1.0 mg cm^{-2}. After assembly, cyclic voltammetry (CV) measurements were performed between 0.005 and 3 V by using an Autolab PGSTAT 302 N (Metrohm) workstation with a scan rate of 0.1 mV s^{-1}. The galvanostatic charge/discharge measurements were carried out between 0.005 and 3.0 V on a Land CT2001A (China). Electrochemical impedance spectroscopy (EIS) measurements were also carried out at the same electrochemical workstation with an amplitude of 10 mV and a frequency ranging from 10 kHz to 0.1 Hz.

3 RESULTS AND DISCUSSION

The fabrication process of N-CTs is schematically illustrated in Fig. 1. Owing to the oxidization and cyclization reactions, dopamine molecules joined via aryl–aryl linkages and forming a polydopamine coating layer on the surface of SiO_2 NFs template in the dispersion process.

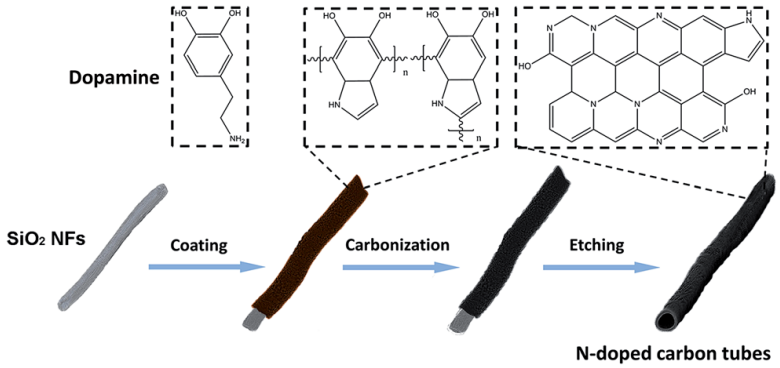

Figure1. Schematic illustration of the synthesis of N-CTs.

3.1 The structure and morphology of N-CTs

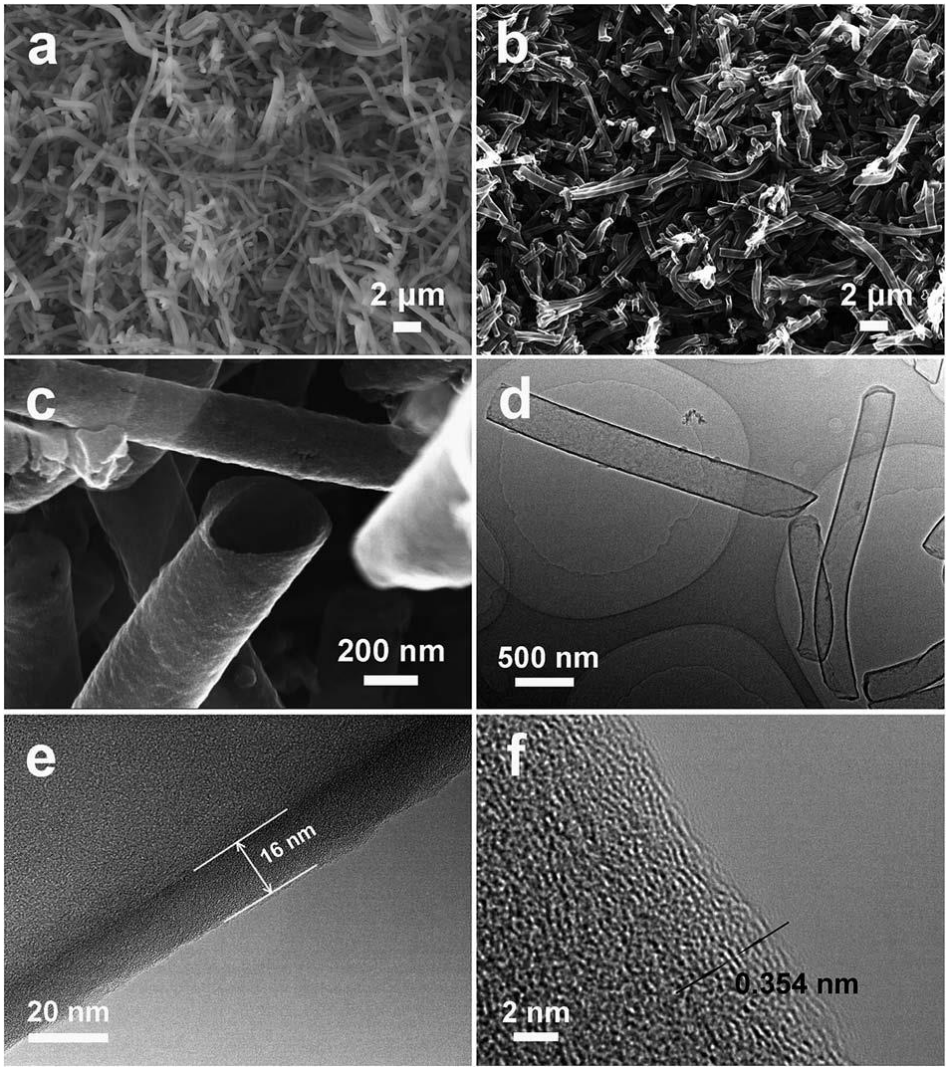

Figure2. (a) SEM image of SiO_2 NFs; (b)(c) SEM image of N-CTs; (d-f) HR-TEM image of N-CTs

The as-prepared N-CTs maintained the one-dimensional skeleton structure of SiO_2 NFs template (Fig. 2a and b) and showed a diameter of 250-400nm with several micrometers in length(Fig. 2c and d), hollow structure could be clearly seen with a uniform wall thickness of ~16nm(Fig. 2e), which was

believed to achieve better wetting and infiltration of electrolyte and shorten the Li^+-diffusion distance[20].And from Fig. 2f, graphitic structure is observed with a interlayer spacing of ~0.354nm, which is slightly larger than that of graphite(0.335nm), the enlarged d-spacing would facilitate intercalation/extraction of Li^+ and increase the reversible capacity.

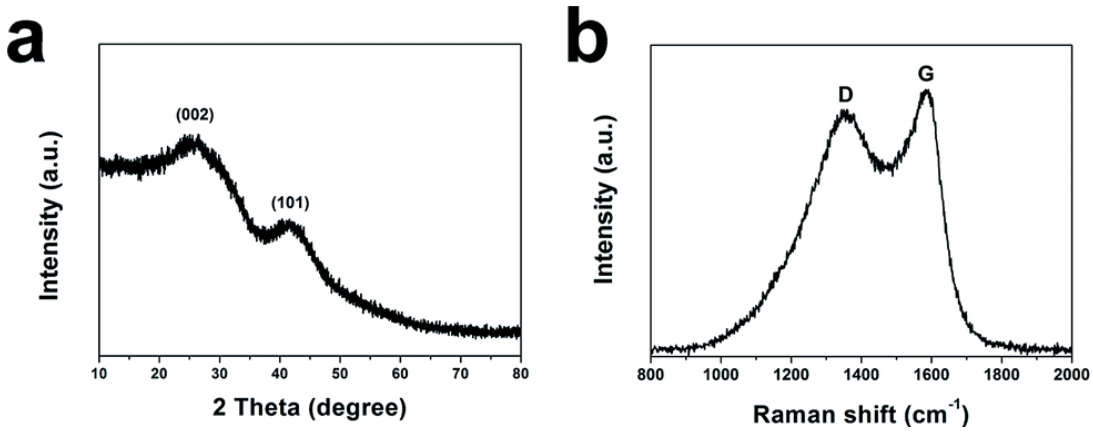

Figure3. XRD pattern(a) and Raman spectrum(b) of N-CTs

Two broad peaks were detected in XRD measurement(Fig. 3a), which reflected the low graphitization degree of N-CTs and consistent with the result of larger interlayer spacing. Further, as shown in Fig. 3b, the N-CTs have two characteristic Raman peaks, D-band located at 1338 cm^{-1} corresponded to the disoredered mode and G-band located at 1590 cm^{-1} corresponded to the stretching mode of C–C bonds of graphite[35], I_D/I_G is about 0.9, further demonstrating the low graphitization degree of N-CTs.

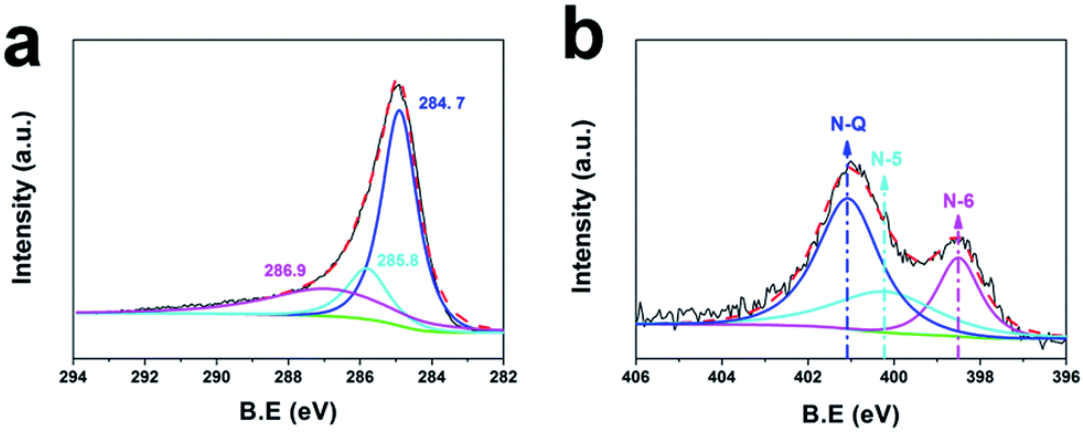

Figure 4. High-resolution XPS of (a) C1s spectrum and (b) N1s spectrum of N-CTs

XPS studies were carried out to demonstrate the in situ doping of nitrogen in the N-CTs. the C1s peak can be resolved into three components located at 284.9, 285.8, and 286.9 eV, which corresponded to sp^2C–sp^2C, N–sp^2C, and N–sp^3C bonds in Figure 4a, respectively. And in Figure 4b, N1s can be deconvoluted into three species: pyridinic N(N-6), pyrrolic N (N-5) and graphitic N (N-Q). Among them, the graphitic N content is abundant (~3.1%). Many defects would be introduced due to the formation of pyridinic and pyrrolic N, which can act as active sites and effectively capture Li-ion.

3.2 The Electrochemical performance of N-CTs as anode for LIBs

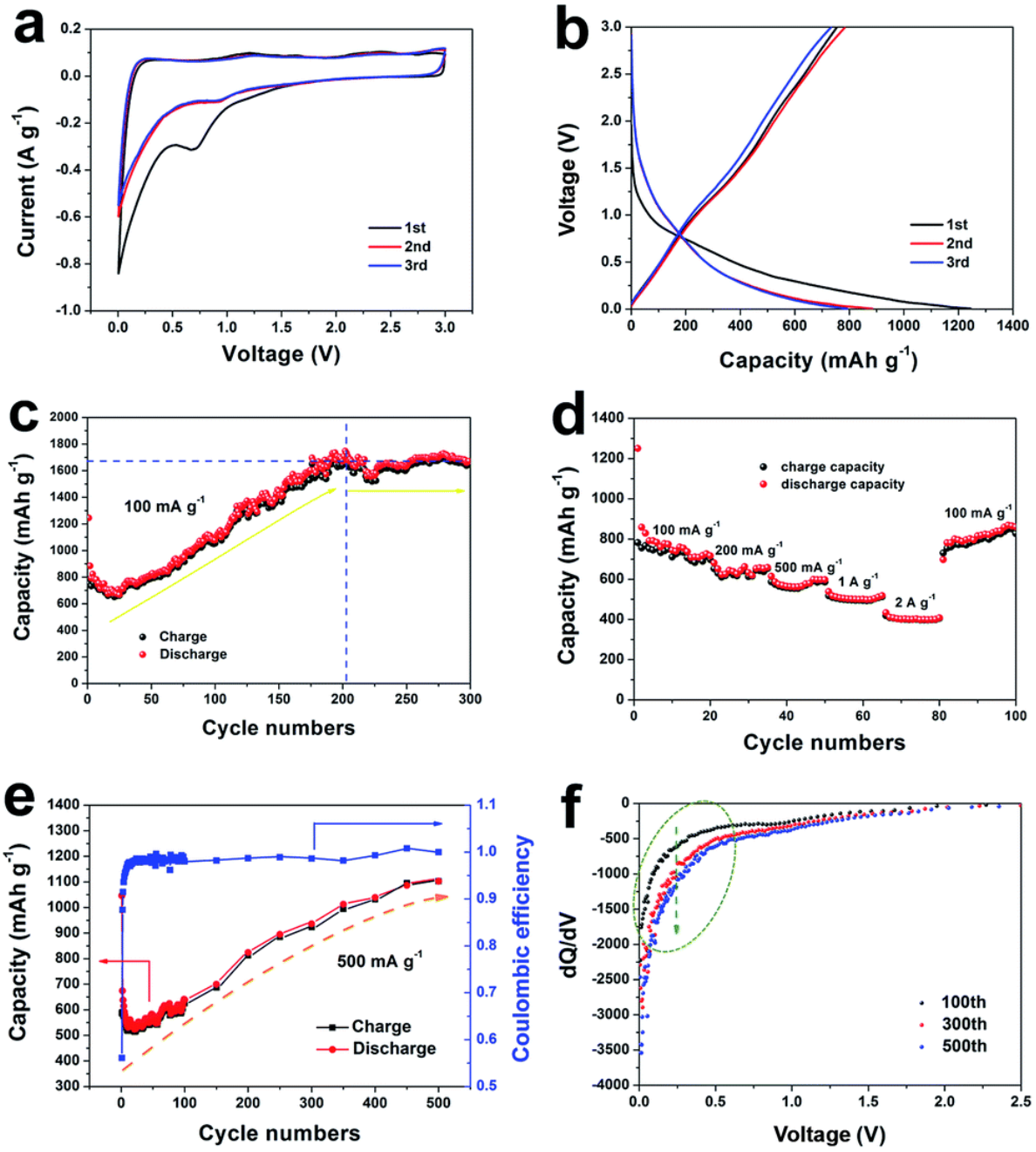

Figure 5. Electrochemical characteristics of the N-CT electrode: (a) first three CV curves at a scan rate of 0.1 mV s^{-1}, (b) first three galvanostatic charge–discharge curves at a rate of 100 mA g^{-1}, (c) cycling performance at 100 mA g^{-1}, (d) rate performance at different rates, (e) long-term cycling performance at a rate of 500 mA g^{-1}, and (f) differential capacity vs. cell voltage.

From CV and charge–discharge curves (Fig. 5a and b), there are no obvious redox peaks and voltage platform, which represents multiple lithium storage behavior of the N-CT electrode. In the potential region below 0.5V, the capacity could be attributed to the lithium insertion into the graphitic layers, the disorder stacking of which may result in the appearance of potential slope. The capacity from 0.8V to 2.0V may result from Li^+ uptake by defects and the capacity from 2.0V to 3.0V is due to

the integration between Li^+ and nitrogen heteroatoms[36]. The first discharged and discharged capacities are 1244.8 and 753.8 mA h g^{-1}, the coulombic efficiency is calculated to be about 60%. The irreversible capacity is mainly caused by the formation of solid electrolyte interphase. As shown in Fig. 5c, the discharged and discharged capacities decrease during the initial several tens of cycles, then gradually increase and finally stabilized at around 1635 mA h g^{-1}after 200 cycles, which is almost twice as high as the beginning. What's more, it shows excellent rate performance with a capacity of 406 mA h g^{-1} even at a high rate of 2 A g^{-1}(Fig. 5d) attributed to the fast transport of Li^+ into N-CTs caused by the special hollow structure with thin wall. From Fig. 5e, the coulombic efficiency is stabilized at above 98% after 25 cycles and the capacity reaches 1100 mA h g^{-1} at 500th cycle. The differential-capacitance–voltage plot reveals that the increase in lithium-storage capability of N-CTs is mainly from the Li^+ uptake below the voltage of ca. 0.8V (Fig. 5e), which means the lithium insertion into the disordered graphitic layers plays the leading role.

4 CONCLUSIONS

In this study, N-doped carbon tubes were fabricated by pyrolyzing polydopamine using silica nanofibers as templates for the first time. Owing to the synergistic effect of unique hollow structure and abundant N-doping(~3.1%) that shorts the Li^+-diffusion distance and facilitates the electron conductivity. The N-CTs shows high specific capacity of 1635 mA h g^{-1} at a rate of 100 mA g^{-1} after 300 cycles, excellent rate capability of 406 mA h g^{-1} even at a high rate of 2 A $g^{-1}$and robust durability when used as an anode material for LIBs, making it a promising candidate for next-generation LIBs.

ACKNOWLEDGEMENT

The authors acknowledge the financial support from the National Natural Science Foundation of China (No. 51072013, 51272021, 51142004) and Natural Science Foundation of Jiangsu Province (BK20131147).

REFERENCE

[1] Armand M, Tarascon J M. Building better batteries.[J]. Nature, 2008, 451(7179):652-657. (doi: 10.1038/451652a)

[2] Nitta N, Yushin G. High-Capacity Anode Materials for Lithium-Ion Batteries: Choice of Elements and Structures for Active Particles[J]. Particle & Particle Systems Characterization, 2014, 31(3):317–336. (doi: 10.1002/ppsc.201300231)

[3] Mukherjee R, Krishnan R, Lu T M, et al. Nanostructured electrodes for high-power lithium ion batteries[J]. Nano Energy, 2012, 1(4):518–533.(doi: 10.1016/j.nanoen.2012.04.001)

[4] Kaskhedikar N A, Maier J. Lithium Storage in Carbon Nanostructures[J]. Advanced Materials, 2009, 21(25-26):2664-2680. (doi: 10.1002/adma.200901079)

[5] Yehezkel S, Auinat M, Sezin N, et al. Bundled and densified carbon nanotubes (CNT) fabrics as flexible ultra-light weight Li-ion battery anode current collectors[J]. Journal of Power Sources, 2016, 312:109-115.(doi: 10.1016/j.jpowsour.2016.02.026)

[6] Cui L F, Hu L, Choi J W, et al. Light-weight free-standing carbon nanotube-silicon films for anodes of lithium ion batteries[J]. Acs Nano, 2010, 4(7):3671-3678.(doi: 10.1021/nn100619m)

[7] Ji L, Yao Y, Toprakci O, et al. Fabrication of carbon nanofiber-driven electrodes from electrospun polyacrylonitrile/polypyrrole bicomponents for high-performance rechargeable

lithium-ion batteries[J]. Journal of Power Sources, 2010, 195(7):2050-2056.(doi: 10.1016/j.jpowsour.2009.10.021)

[8] Cho J S, Hong Y J, Kang Y C. Design and Synthesis of Bubble-Nanorod-Structured Fe_2O_3-Carbon Nanofibers as Advanced Anode Material for Li-Ion Batteries.[J]. Acs Nano, 2015, 9(4):4026-4035.(doi: 10.1021/acsnano.5b00088)

[9] Chang K, Chen W. L-cysteine-assisted synthesis of layered MoS_2/graphene composites with excellent electrochemical performances for lithium ion batteries[J]. Acs Nano, 2011, 5(6):4720-4728.(doi: 10.1021/nn200659w)

[10] Luo J, Liu J, Zeng Z, et al. Three-dimensional graphene foam supported Fe_3O_4 lithium battery anodes with long cycle life and high rate capability.[J]. Nano Letters, 2013, 13(12):6136-6143.(doi: 10.1021/nl403461n)

[11] Zhou X, Wan L J, Guo Y G. Binding SnO_2, Nanocrystals in Nitrogen-Doped Graphene Sheets as Anode Materials for Lithium-Ion Batteries[J]. Advanced Materials, 2013, 25(15):2152-2157.(doi: 10.1002/adma.201300071)

[12] Tang K, White R J, Mu X, et al. Hollow carbon nanospheres with a high rate capability for lithium-based batteries[J]. Chemsuschem, 2012, 5(2):400-403.(doi: 10.1002/cssc.201100609)

[13] Yang Y, Jin S, Zhang Z, et al. Nitrogen-Doped Hollow Carbon Nanospheres for High-Performance Li-Ion Batteries.[J]. Acs Applied Materials & Interfaces, 2017, 9(16): 14180-14186.(doi: 10.1021/acsami.6b14840)

[14] Chen Y, Li X, Park K, et al. Hollow carbon-nanotube/carbon-nanofiber hybrid anodes for Li-ion batteries.[J]. Journal of the American Chemical Society, 2013, 135(44):16280-16283. (doi: 10.1021/ja408421n)

[15] Chen Y, Lu Z, Zhou L, et al. Triple-coaxial electrospun amorphous carbon nanotubes with hollow graphitic carbon nanospheres for high-performance Li ion batteries[J]. Energy & Environmental Science, 2012, 5(7):7898-7902. (doi: 10.1039/C2EE22085G)

[16] Zhang Z, Wang L, Xiao J, et al. One-Pot Synthesis of Three-Dimensional Graphene/Carbon Nanotube/SnO2 Hybrid Architectures with Enhanced Lithium Storage Properties[J]. Acs Applied Materials & Interfaces, 2015, 7(32):17963-17968. (doi: 10.1021/acsami.5b04673)

[17] Liu J, Liu W, Ji S, et al. Facile Synthesis of Carbon-Encapsulated Li4Ti5O12@C Hollow Microspheres as Superior Anode Materials for Li-Ion Batteries[J]. European Journal of Inorganic Chemistry, 2014, 2014(12):2073-2079. (doi: 10.1002/ejic.201301558)

[18] Zhang K, Li X, Liang J, et al. Nitrogen-doped porous interconnected double-shelled hollow carbon spheres with high capacity for lithium ion batteries and sodium ion batteries[J]. Electrochimica Acta, 2015, 155:174-182. (doi: 10.1016/j.electacta.2014.12.108)

[19] Song H, Li N, Cui H, et al. Enhanced storage capability and kinetic processes by pores- and hetero-atoms- riched carbon nanobubbles for lithium-ion and sodium-ion batteries anodes[J]. Nano Energy, 2014, 4(3):81-87. (doi: 10.1016/j.nanoen.2013.12.017)

[20] Wang Z L, Xu D, Wang H G, et al. In Situ Fabrication of Porous Graphene Electrodes for High-Performance Energy Storage[J]. Acs Nano, 2013, 7(3):2422-2430. (doi: 10.1021/nn3057388)

[21] Qie L, Chen W M, Wang Z H, et al. Nitrogen-doped porous carbon nanofiber webs as anodes for lithium ion batteries with a superhigh capacity and rate capability[J]. Advanced Materials, 2012, 24(15):2047-2050. (doi: 10.1002/adma.201104634)

[22] Liu X, Wu Y, Yang Z, et al. Nitrogen-doped 3D macroporous graphene frameworks as anode

for high performance lithium-ion batteries[J]. Journal of Power Sources, 2015, 293:799-805. (doi: 10.1016/j.jpowsour.2015.05.074)

[23] Hou Y, Li J, Wen Z, et al. Co 3 O 4, nanoparticles embedded in nitrogen-doped porous carbon dodecahedrons with enhanced electrochemical properties for lithium storage and water splitting[J]. Nano Energy, 2015, 12:1-8. (doi: 10.1016/j.nanoen.2014.11.043)

[24] Li X, Zhu X B, Zhu Y, et al. Porous nitrogen-doped carbon vegetable-sponges with enhanced lithium storage performance[J]. Carbon, 2014, 69(2):515-524.(doi: 10.1016/j.carbon.2013.12.059)

[25] Han P, Yue Y, Zhang L, et al. Nitrogen-doping of chemically reduced mesocarbon microbead oxide for the improved performance of lithium ion batteries[J]. Carbon, 2012, 50(3):1355-1362. (doi: 10.1016/j.carbon.2011.11.007)

[26] Yan X, Liu Y, Fan X, et al. Nitrogen/phosphorus co-doped nonporous carbon nanofibers for high-performance supercapacitors[J]. Journal of Power Sources, 2014, 248(248):745-751. (doi: 10.1016/j.jpowsour.2013.09.129)

[27] Ryou M H, Lee Y M, Park J K, et al. Mussel-inspired polydopamine-treated polyethylene separators for high-power li-ion batteries[J]. Advanced Materials, 2011, 23(27):3066-3070. (doi: 10.1002/adma.201100303)

[28] Wang L, Dong Z, Wang D, et al. Covalent Bond Glued Sulfur Nanosheet-Based Cathode Integration for Long-Cycle-Life Li-S Batteries[J]. Nano Letters, 2013, 13(12):6244-6250. (doi: 10.1021/nl403715h)

[29] Xie W, Li S, Wang S, et al. N-Doped Amorphous Carbon Coated Fe3O4/SnO2 Coaxial Nanofibers as a Binder-Free Self-Supported Electrode for Lithium Ion Batteries.[J]. Acs Applied Materials & Interfaces, 2014, 6(22):20334-20339. (doi: 10.1021/am505829v)

[30] Kong J, Yee W A, Yang L, et al. Highly electrically conductive layered carbon derived from polydopamine and its functions in SnO2-based lithium ion battery anodes.[J]. Chemical Communications, 2012, 48(83):10316-10318. (doi: 10.1039/c2cc35284b)

[31] Wang Y, Ding X, Wang F, et al. Nanoconfined nitrogen-doped carbon-coated MnO nanoparticles in graphene enabling high performance for lithium-ion batteries and oxygen reduction reaction[J]. Chemical Science, 2016, 7(7):4284-4290. (doi: 10.1039/C5SC04668H)

[32] Ming C, Xiao S, Chen K, et al. Nitrogen-doped Mesoporous Carbon-encapsulation Urchin-like Fe_3O_4, as Anode Materials for High Performance Li-ions Batteries[J]. Electrochimica Acta, 2016, 195:94-105. (doi: 10.1016/j.electacta.2016.02.128)

[33] Lei C, Han F, Li D, et al. Dopamine as the coating agent and carbon precursor for the fabrication of N-doped carbon coated Fe3O4 composites as superior lithium ion anodes[J]. Nanoscale, 2013, 5(3):1168-1175. (doi: 10.1039/c2nr33043a)

[34] Liu Y, Sagi S, Chandrasekar R, et al. Preparation and characterization of electrospun SiO2 nanofibers.[J]. Journal of Nanoscience & Nanotechnology, 2008, 8(3):1528-1536. (doi: 10.1166/jnn.2008.043)

[35] Han F D, Bai Y J, Liu R, et al. Template-Free Synthesis of Interconnected Hollow Carbon Nanospheres for High-Performance Anode Material in Lithium-Ion Batteries[J]. Advanced Energy Materials, 2011, 1(5):798-801. (doi: 10.1002/aenm.201100340)

[36] Hu C, Wang L, Zhao Y, et al. Designing nitrogen-enriched echinus-like carbon capsules for highly efficient oxygen reduction reaction and lithium ion storage[J]. Nanoscale, 2014, 6(14):8002-8009. (doi: 10.1039/c4nr01184h)